Theoretical investigation of the bonding and solubility in $Nb_{2-x}W_xAlC$

2005 J. Phys.: Condens. Matter 17 6047

(http://iopscience.iop.org/0953-8984/17/38/010)

INSTITUTE OF PHYSICS PUBLISHING JOURNAL OF PHYSICS: CONDENSED MATTER

J. Phys.: Condens. Matter **17** (2005) 6047–6056 doi:10.1088/0953-8984/17/38/010

Theoretical investigation of the bonding and solubility in $Nb_{2-x}W_xAlC$

Jochen M Schneider[1], **Zhimei Sun and Denis Music**

Materials Chemistry, RWTH Aachen, Kopernikusstrasse 16, D-52074 Aachen, Germany

E-mail: schneider@mch.rwth-aachen.de

Received 21 April 2005, in final form 19 July 2005
Published 9 September 2005
Online at stacks.iop.org/JPhysCM/17/6047

Abstract

We have performed theoretical studies of the solubility within $Nb_{2-x}W_xAlC$ by means of *ab initio* total energy calculations. If x is increased from 0 to 2 the bulk modulus can be increased by as much as 31%. The bulk modulus deviates from Vegard's rule, which may be understood based on substitution-induced changes in the $CNb_{2-x}W_x$ bond angle resulting in flattening of the $Nb_{2-x}W_xC$ layers upon solid solution formation. This rather extensive increase in the bulk modulus can be understood by considering the changes caused by the substitution of Nb through W for the equilibrium volume and chemical bonding. Based on the energy of formation analysis we suggest that the investigated system shows complete solubility. The bond length calculations suggest that both the Nb–C bond length as well as the W–C bond length are not significantly affected by variations in x. Based on a comparison to other solid solutions we suggest that this anomaly may be specific to the family of nanolaminates investigated here.

1. Introduction

M_2AX phases, where M is an early transition metal, A is an A group element and X is either C and/or N, exhibit a layered hexagonal structure which can be described as MX layers interleaved with A layers, and are therefore also referred to as nanolaminates [1]. These compounds can generally be characterized as good thermal and electrical conductors [2, 3], they are machinable [2], and they exhibit high stiffness as well as high strength at elevated temperatures [2, 4]. In addition it was reported that these materials also demonstrate good thermal shock and oxidation resistance [2, 5–7]. This combination of properties is rather unusual and is responsible for the growing academic and technological attention given to MAX phases recently.

[1] Author to whom any correspondence should be addressed.

Varying the chemical composition of a solid solution is an efficient way to tune material properties. The information available on the mutual solubility among M_2AX phases is limited. The formation of $(Ti, V)_2SC$ [8] and $(Nb, Zr)_2AlC$ [9] has been discussed. Pietzka and Schuster [10] reported the existence of $Ti_2AlC_{0.82-x}N_x$ at 1490 °C, where $x = 0$–0.8; Schuster *et al* [11] investigated the mutual solutions between Ti_2AlC, V_2AlC, and Cr_2AlC by annealing series of powder mixtures in proportions 25, 50 and 75 mol% at 1000 °C for 170 h in evacuated sealed quartz tubes. Their experimental results showed that V_2AlC formed a complete series of mutual solutions with Cr_2AlC and Ti_2AlC, while the mutual solution series of Ti_2AlC–Cr_2AlC exhibited a miscibility gap which the authors attributed to the relatively high solubility of Cr_3C_2 in TiC_{1-x} competing with the solution stability and the larger size difference of the metal atoms. Recently, Hug *et al* [12] demonstrated good agreement for the investigation of the electronic structure between x-ray absorption spectroscopy and full-potential augmented plane wave calculations for several MAX phases, including the solid solution of $(Ti_{0.5}Nb_{0.5})_2AlC$. Systematic theoretical studies of mutual substitutions of the transition metals in M_2AlC phases for the neighbouring elements, Ti, V and Cr by means of *ab initio* total energy calculations are available in the literature [13, 14]. Sun *et al* [13] discussed the effect of valence electron increase on the bulk modulus and solubility: based on the total density of states analysis as well as the energy of formation all investigated solution systems showed total solubility except for the $(Cr, Ti)_2AlC$ system. These calculations are consistent with published experimental solubility data [11]. Wang *et al* reported the effect of the valence electron concentration on the elastic constants: C_{44} reaches a maximum at valence electron concentrations of 8.4–8.6 which was argued to be due to filling of shear resistive p–d bonging states [14]. This band filling argument is consistent with earlier work of Sun *et al* for the system M_2AlC with M = (Ti, V, and Cr) [13, 15]. Recently, we have investigated the correlation between chemical bonding and bulk modulus for 31 known and 5 hitherto unknown M_2AC phases with M = (Ti, Zr, Hf, V, Nb, Ta, Cr, Mo, W) and A = (Al, Ga, Ge, Sn) [16]. In this work the bulk modulus of W_2AlC was estimated to be 265 GPa, which is close to that of α-Al_2O_3 [17] and would to our knowledge constitute the highest bulk modulus of this class of materials. The synthesis of this material has so far not been reported in the literature. In the same work the bulk modulus of Nb_2AlC was estimated to be 203 GPa. The formation of Nb_2AlC has been reported in bulk form by Salama and co-workers [18]. The aim of the present work is to theoretically investigate the solubility of $Nb_{2-x}W_xAlC$. It is our ambition to contribute towards a better basic understanding of this fascinating class of materials and initiate experimental investigations.

2. Calculation methods and structure constructions

The present calculations are based on the density functional theory at 0 K, using the so-called VASP [19, 20] program package in conjunction with generalized-gradient approximations projector augmented wave potentials [21]. The following parameters are used in our calculations: the relaxation convergence for ions was 1×10^{-4} eV, the electronic relaxation convergence was 1×10^{-5} eV, conjugate gradient optimization of the wavefunctions, reciprocal-space integration with a Monkhorst–Pack scheme [22], energy cutoff of 500 eV, k-points grid of $7 \times 7 \times 7$ and the tetrahedron method with Blöchl corrections for the energy [23]. To study the solution $Nb_{2-x}W_xAlC$ structures, supercells with 16 atoms ($2 \times c$) were first constructed so as to obtain 25, 50, 75 at.% of W in Nb_2AlC. The supercells were then fully relaxed and the total energy was calculated at various cell volumes with the $P6_3/mmc$ symmetry. The calculated data were then fitted to the third-order Birch–Murnaghan's equations of state [24] to extract the equilibrium volume (V_0), the bulk modulus (B) and the pressure derivative of B. The total-energy calculations have been made for the constituents in their equilibrium

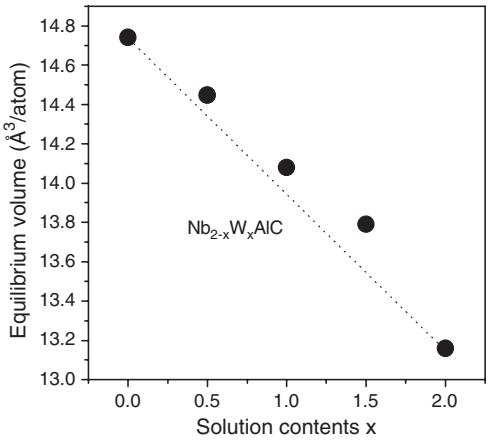

Figure 1. The calculated equilibrium volume of $Nb_{2-x}W_xAlC$ as a function of the solution content x. The dotted line follows the prediction from Vegard's rule.

Table 1. Calculated and experimental structure parameters, and the bulk moduli calculated from equations of state, as well as the optimized free internal parameter, $z(M)$. Herein a and c are the lattice constants, and V_0, B and B' are the equilibrium volume, the bulk modulus and its pressure derivative, respectively.

	a (Å)	c (Å)	V_{VASP} (Å^3)	V_{EXP} (Å^3)	$z(M)$	B (GPa)	B'
NbC	4.468	—	89.195	89.315[a]	—	201	4.20
Nb_2AlC	3.129	13.894	117.936	116.031[b]	0.091	203	4.30
$Nb_{1.5}W_{0.5}AlC$	3.116	13.744	115.576	—	0.093	214	4.13
$Nb_{1.0}W_{1.0}AlC$	3.079	13.711	112.632	—	0.090	228	4.26
$Nb_{0.5}W_{1.5}AlC$	3.049	13.714	110.392	—	0.091	242	4.29
W_2AlC	2.954	13.845	105.272	—	0.097	265	4.37
WC	4.265	—	77.584	—	—	265	4.20

[a] See reference [29].
[b] See reference [18].

structures to evaluate the (E_{form}) energy of formation:

$$E_{form} = \frac{E(Nb_{2-x}W_xAlC) - 4(2-x)E(Nb) - 4xE(W) - 4E(Al) - 4E(graphite)}{16}. \quad (1)$$

Finally, from these total-energy calculations Fermi energies (E_F), bond lengths, and charge density distributions and partial density of states were extracted.

3. Results and discussions

3.1. Equilibrium volume and bulk modulus calculated from equations of state

The calculated and experimental cell parameters, the bulk moduli calculated from the equations of state, as well as the optimized free internal parameter, are given in table 1. Our estimated equilibrium volume for Nb_2AlC and the lattice parameters agree well with the experimental data [18]; the difference in equilibrium volume is 1.6%. For W_2AlC as well as for all investigated quaternary phases no experimental data are available. The calculated values of equilibrium volume as a function of the solution contents x are shown in figure 1. As Nb is replaced with W, the equilibrium volume decreases by 10.7% from 117.936 to 105.272 Å^3.

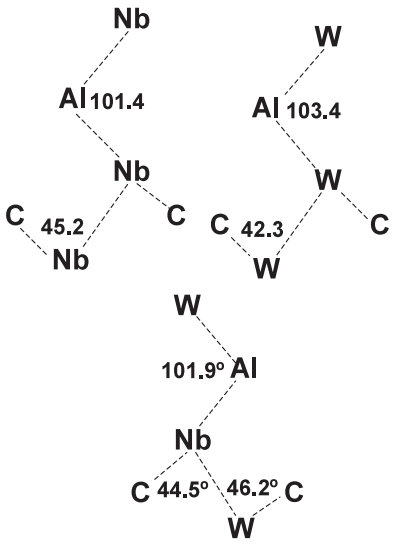

Figure 2. Bond angle data for Nb_2AlC, W_2AlC and NbWAlC.

A positive deviation from Vegard's rule can be observed: the maximum increase in volume is 1.7% for $Nb_{0.5}W_{1.5}AlC$. This deviation from Vegard's rule can be understood based on alterations in bond angles and consequently lattice parameters. In figure 2 the bond angle data for Nb_2AlC, W_2AlC and NbWAlC are given. The C–Nb–Nb angle in Nb_2AlC is 45.2°, while the corresponding angle in W_2AlC is 42.3°, which constitutes a 6.6% decrease. As Nb is substituted by W to form the NbWAlC solid solution, the corresponding angle is 46.2°. Furthermore, there are no significant changes in Nb_{2-x}–Al–W_x bond angles: the Nb–Al-Nb angle in Nb_2AlC is 101.4°, while the corresponding angle in W_2AlC is 103.4°, which constitutes a 2.0% increase. As Nb is substituted by W to form NbWAlC, the corresponding angle is 101.9°. An increase in the $CNb_{2-x}W_x$ bond angle is consistent with the notion of flattening of the $Nb_{2-x}W_xC$ layers and hence an increase in the a-lattice parameter, while the increase in Nb_{2-x}–Al–W_x bond angle corresponds to an increase in the c-lattice parameter (see table 1). For NbWAlC, a and c lattice parameters deviate by +1.2% and −1.1% from Vegard's rule, respectively. Since the volume is proportional to a^2 and c, the flattening of the $Nb_{2-x}W_xC$ layers is the dominating atomic mechanism causing positive deviations in volume from Vegard's rule. In figure 3 the theoretical bulk moduli are shown as a function of solution content x. The deviation from linearity is consistent with the deviation from Vegard's rule discussed above. As x is varied from 0 to 2 the bulk modulus of the solution can be varied by 30.5% from 203 to 265 GPa, which may be understood by changes in chemical bonding: these are indicated in table 2, providing the Fermi energy (E_F) of the solution compounds as a function of x. It can be seen that the gradual substitution of Nb by W increases the valence electron concentration, and correspondingly E_F moves to a higher energy level, which can be understood by extra valence electrons filling the p–d hybridized bonding states. This is consistent with previous work [15]. The effect of the substitution can be seen in figure 4, where charge density distributions for Nb_2AlC, NbWAlC and W_2AlC are given, and in figure 5, where the partial density of states is provided for the same compounds. This band filling in turn results in an increase in bond strength, and hence an increase in bulk moduli. As Nb is replaced with W, more charge is placed in the M–C bonds, which is due to an increase in the C p–M d

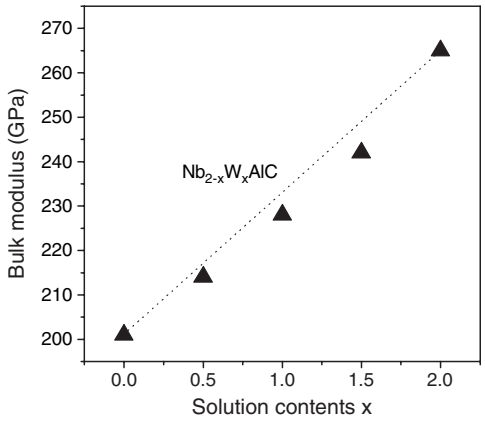

Figure 3. The calculated bulk moduli of $Nb_{2-x}W_xAlC$ as a function of the solution content x. The dotted line follows the prediction from Vegard's rule.

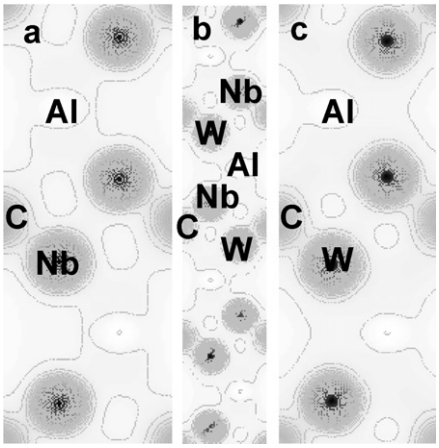

Figure 4. Charge density distribution in the $(11\bar{2}0)$ plane for (a) Nb_2AlC, (b) NbWAlC and (c) W_2AlC. The electron density increases from 0 (white) to 5.2 electrons $Å^{-3}$ (grey), with the step of 0.2 electrons $Å^{-3}$.

hybridization. The hybridized C 2p–M d states dominate the bonding. Another difference in bonding between the Nb_2AlC and W_2AlC structures is the weakly hybridized Al 3p–M d states which are around −2 and −3 eV for Nb_2AlC and W_2AlC, respectively. This indicates that the Nb–Al bond is indeed weaker than the W–Al bond. This is expected, considering the classification system proposed by Sun *et al* [16], where M_2AC phases with a transition metal of group V and larger are characterized by strong coupling between the MC and A layers as well as by strong coupling between adjacent MC layers. In these solids MC bonding of the binary carbide is conserved in the ternary compound although A layers are interleaved with MC layers [16].

3.2. Bond length data

The bond length data for $Nb_{2-x}W_xAlC$ are readily available from our *ab initio* calculations, which suggest that both the Nb–C bond length and the W–C bond length are not significantly

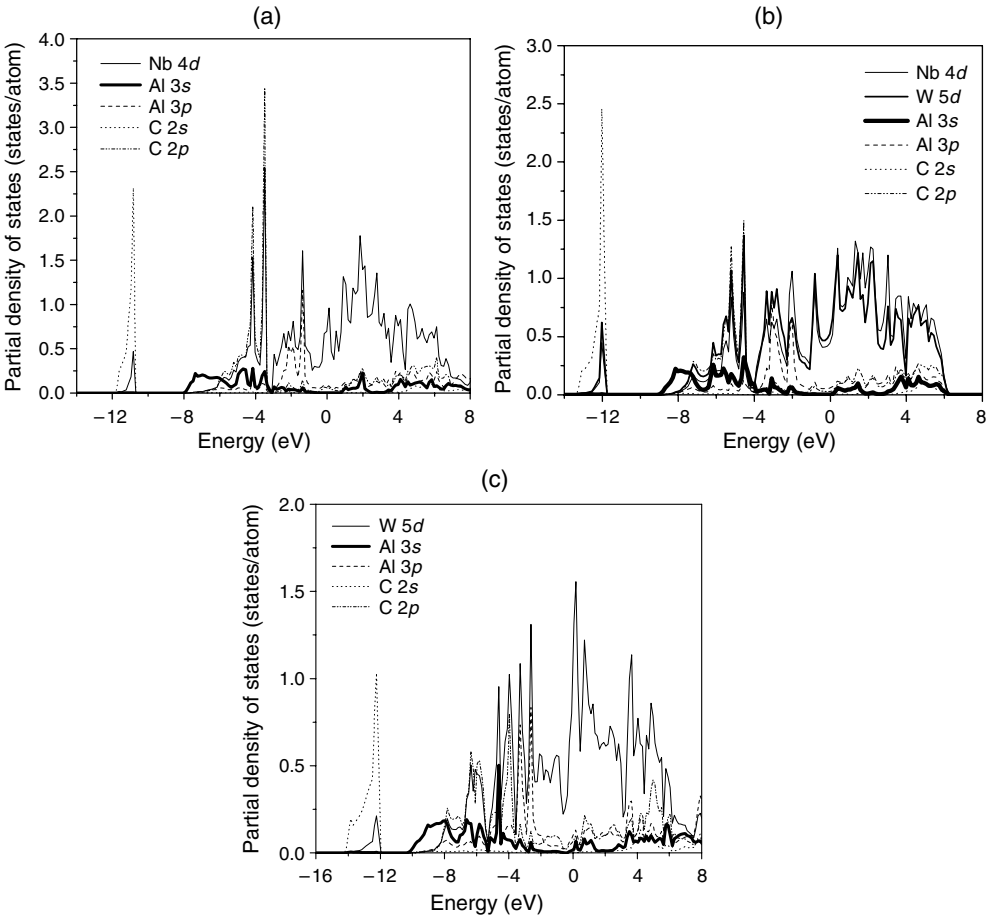

Figure 5. Partial density of states for (a) Nb_2AlC, (b) NbWAlC and (c) W_2AlC, as obtained by the VASP code. Fermi level is set to 0 eV.

Table 2. The calculated bond lengths and Fermi energies (E_F) for the solid solution $Nb_{2-x}W_xAlC$, ternary carbides Nb_2AlC and W_2AlC and the binary carbides NbC and WC as well as energy of formation differences between all MAX phases to the mechanical mixture (ΔE_{form}).

	Nb–C (Å)	Nb–Al (Å)	W–C (Å)	W–Al (Å)	E_F (eV)	ΔE_{form} (eV/atom)
NbC	2.23				—	—
Nb_2AlC	2.21	2.86			6.29	0
$Nb_{1.5}W_{0.5}AlC$	2.19	2.85	2.13	2.78	6.39	−0.09
$Nb_{1.0}W_{1.0}AlC$	2.19	2.84	2.13	2.78	6.61	−0.08
$Nb_{0.5}W_{1.5}AlC$	2.20	2.87	2.14	2.79	6.88	−0.05
W_2AlC			2.13	2.73	8.55	0
WC			2.13		—	—

affected by variations in x. This is shown in figure 6(a). The relative changes in bond length and volume are given in figure 6(b). It is evident that significant changes occur in the equilibrium volume and not in the bond length. In fact, comparing the transition metal carbide bond

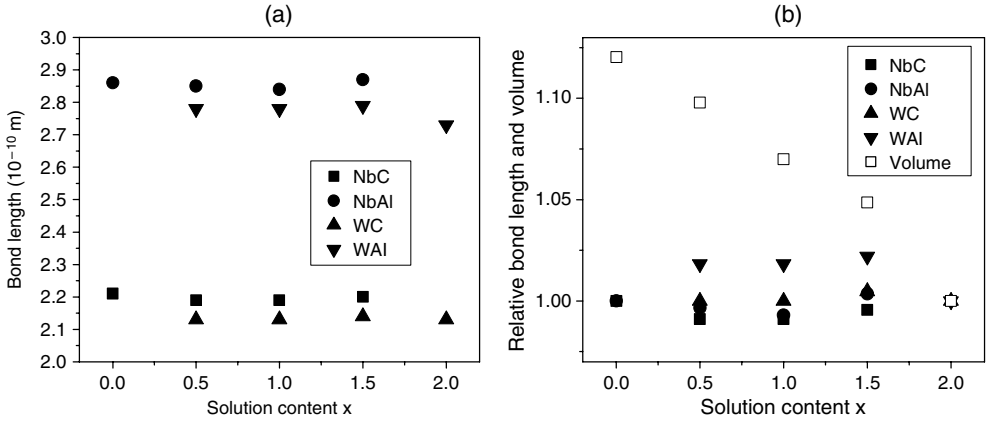

Figure 6. (a) Nb–C, W–C, Nb–Al and W–Al bond length data of $Nb_{2-x}W_xAlC$ as a function of the solution content x. (b) Relative Nb–C, W–C, Nb–Al and W–Al bond lengths and relative volume of $Nb_{2-x}W_xAlC$ as a function of the solution content x.

distances of the MAX phases investigated here to the bond length of the binary transition metal carbide results in a bond length difference of $\leqslant 0.9\%$, while the changes due to variation of x are also $\leqslant 0.9\%$. Furthermore, the bond length data for Nb–Al and W–Al are also not significantly affected by variations in x. Hence, the considerable variation in unit volume which is caused by x is due to the varying amount of Nb and W based bonds and not due to a change in bond lengths of the individual Nb and W based bonds. This behaviour is unusual: it is expected that the bond length is affected by chemical composition when solid solutions are formed, because substituting A in a system A–B–C with D should affect the electron density distribution of the D–B bonds as well as the D–C bonds. This behaviour has been observed in simple wurzite $(Ga_xIn_{1-x})_2Se_3$ [25], and perovskite $La_{1-x}Sr_xMnO_3$ [26] as well as in layered structures such as $Li_x(Ni_{0.5}Mn_{0.5})O_2$ [27] and $Li_x(Mn_{1-y}Co_y)O_2$ [28]. This, however, is not the case for the $Nb_{2-x}W_xAlC$ solid solution studied here.

As discussed previously, the information available on the mutual solubility among M_2AX phases is limited: while systematic theoretical studies of mutual substitutions of the transition metals in M_2AlC phases for the neighbouring elements, Ti, V and Cr, by means of *ab initio* total energy calculations are available in the literature [13, 14], the effect of the chemical composition on the bond length has not been discussed. Hence, we have revisited our solubility calculations for M_2AlC [13] with M = Ti, V and Cr. The bond length data are given in table 3. The calculations suggest that in the systems M_2AlC with M = Ti, V and Cr, the Ti–C, V–C and Cr–C bond lengths are also not significantly affected by variations in x (see figure 7). Comparing the transition metal carbide bond distances of the ternary transition metal aluminium carbides investigated here to the bond length of the corresponding binary transition metal carbide results in a bond length difference of $\leqslant 3.9\%$, while the changes due to variation of x are also $\leqslant 2.0\%$. These deviations are comparable to the previously discussed deviations in the system $Nb_{2-x}W_xAlC$. We therefore suggest that this anomaly with respect to other material systems [25–28] may be specific to the family of nanolaminates investigated here. This strikingly surprising phenomenon can be understood considering the partial density of states and the charge density distribution. C forms strong bonds with Nb and W, which can be seen in figure 4, where charge density distributions for Nb_2AlC, NbWAlC and W_2AlC are given, and in figure 5, where the partial density of states is provided for the same compounds. As WC units are introduced into a Nb_2AlC matrix to form NbWAlC, no significant change in

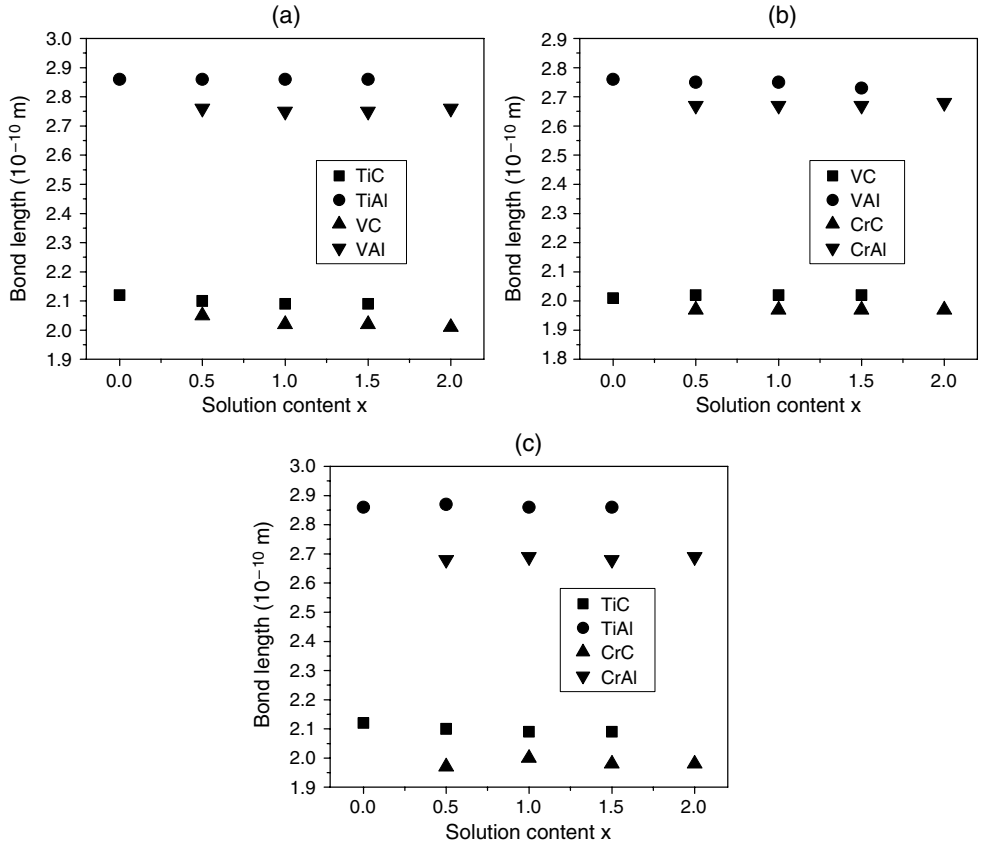

Figure 7. (a) Ti–C, V–C, Ti–Al and V–Al bond length data of $Ti_{2-x}V_xAlC$, (b) V–C, Cr–C, V–Al and Cr–Al bond length data of $V_{2-x}Cr_xAlC$ and (c) Cr–C, Ti–C, Cr–Al and Ti–Al bond length data of $Cr_{2-x}Ti_xAlC$ as a function of the solution content x.

the hybridization between W 5d and C 2p as well as Nb 4d and C 2p states can be observed, suggesting that the bonding between transition metal and C is fact conserved while x is varied. Furthermore, it is evident that the interaction between W 5d and Nb 4d states is weak, despite the proximity of Nb and W.

3.3. Energy of formation

To study the relative phase stabilities, we have calculated the energy of formation versus x. The energy of formation differences of all quaternary compounds to the mechanical mixture are negative, indicating a stable solid solution (see figure 8 and table 2). At $T > 0$ K the stability depends on the Gibbs free energy and hence a contribution of enthalpy and entropy. We base our stability discussion on calculated enthalpy differences at 0 K. The contributions of entropy as well as the temperature dependence of the enthalpy have to be included in the discussion in order to determine the actual phase stabilities at temperature $T > 0$ K. However, our previous calculations [13] of the solubility within $(M_xM'_{2-x})AlC$, where M and M′ = Ti, V and Cr, was consistent with the published experimental solubility data [11]. The magnitude of the energy of formation difference of two previously investigated $M_xM'_{2-x}AlC$ systems with M = V and M′ = Ti and Cr to the mechanical mixture thereof is comparable to the

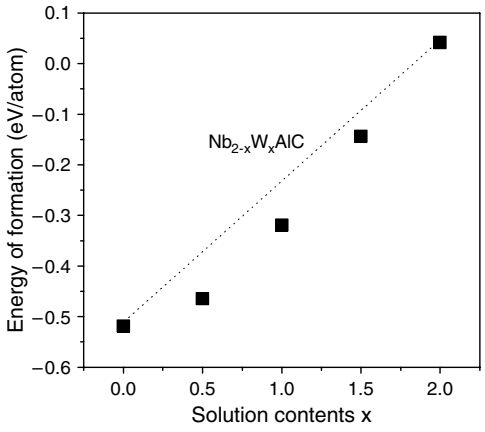

Figure 8. The calculated energy of formation of $Nb_{2-x}W_xAlC$ as a function of the solution content x. The dotted line follows the prediction from Vegard's rule.

Table 3. The calculated bond lengths for the solid solutions $Ti_{2-x}V_xAlC$, $Ti_{2-x}Cr_xAlC$ and $V_{2-x}Cr_xAlC$, ternary carbides Ti_2AlC, V_2AlC and Cr_2AlC as well as energy of formation differences between all MAX phases to the mechanical mixture (ΔE_{form}). The relaxed structures stem from our previous work [13].

	Ti–C (Å)	Ti–Al (Å)	V–C (Å)	V–Al (Å)	Cr–C (Å)	Cr–Al (Å)	ΔE_{form} (eV/atom)
TiC	2.16						—
Ti_2AlC	2.12	2.86					0.00
$Ti_{1.5}V_{0.5}AlC$	2.10	2.86	2.05	2.76			−0.02
$Ti_{1.0}V_{1.0}AlC$	2.09	2.86	2.02	2.75			−0.03
$Ti_{0.5}V_{1.5}AlC$	2.09	2.86	2.02	2.75			−0.04
VC			2.08				—
V_2AlC			2.01	2.76			0.00
$V_{1.5}Cr_{0.5}AlC$			2.02	2.75	1.97	2.67	−0.03
$V_{1.0}Cr_{1.0}AlC$			2.02	2.75	1.97	2.67	−0.02
$V_{0.5}Cr_{1.5}AlC$			2.02	2.73	1.97	2.67	−0.01
CrC					2.05		—
Cr_2AlC					1.97	2.68	0.00
$Ti_{1.5}Cr_{0.5}AlC$	2.10	2.87			2.00	2.69	0.00
$Ti_{1.0}Cr_{1.0}AlC$	2.09	2.86			1.98	2.68	0.00
$Ti_{0.5}Cr_{1.5}AlC$	2.09	2.86			1.98	2.69	0.00

corresponding difference for the $Nb_{2-x}W_xAlC$ solid solution studied here. Furthermore, the energy of formation of W_2AlC was investigated and we find 0.04 eV/atom, suggesting that the W_2AlC phase is metastable compared to the pure elements. However, the energy of formation data presented above for $Nb_{2-x}W_xAlC$ with $x = 0.5$–1.5 suggest total solubility.

4. Conclusions

We have performed theoretical studies of the solubility within $Nb_{2-x}W_xAlC$ by means of *ab initio* total energy calculations. If x is increased from 0 to 2 the bulk modulus can be increased by as much as 31%. The bulk modulus deviates from Vegard's rule, which may be understood based on substitution-induced changes in the $CNb_{2-x}W_x$ bond angle, resulting

in flattening of the $Nb_{2-x}W_xC$ layers upon solid solution formation. This rather extensive increase can be understood by considering the changes caused by the substitution of Nb by W for the equilibrium volume and chemical bonding. Based on the energy of formation analysis we suggest that the investigated system shows complete solubility. Hence, the solid solution synthesis route may be a pathway towards the synthesis of MAX phases with a stiffness similar to α-Al_2O_3. Furthermore, we show that the Nb–C and W–C bond length in $Nb_{2-x}W_xAlC$ is not significantly affected by chemical composition. This behaviour is also observed for three other carbide-based MAX phase solid solutions. We therefore suggest that this anomaly may be specific to the family of nanolaminates investigated here.

Acknowledgments

JMS acknowledges sponsorship of the Alexander von Humboldt Foundation, the Federal Ministry of Education and Research and the Program for Investment in the Future. We also acknowledge support from the Swedish Research Council.

References

[1] Barsoum M W 2000 *Prog. Solid State Chem.* **28** 201
[2] Barsoum M W and El-Raghy T 1996 *J. Am. Ceram. Soc.* **79** 1953
[3] Sun Z and Zhou Y 2000 *Phys. Rev.* B **60** 1441
[4] Sun Z, Zhou Y and Zhou J 2000 *Phil. Mag. Lett.* **80** 289
[5] El-Raghy T, Barsoum M W, Zavaliangos A and Kalidini S 1999 *J. Am. Ceram. Soc.* **82** 2855
[6] Barsoum M W, El-Raghy T and Ogbuji L 1997 *J. Electrochem. Soc.* **144** 2508
[7] Sun Z, Zhou Y and Li S 2001 *Acta Mater.* **49** 4347
[8] Nowotny H, Rogl P and Schuster J 1982 *J. Solid State Chem.* **44** 126
[9] Reiffenstein E, Nowotny H and Benesovsky F 1966 *Monatsh. Chem.* **97** 1428
[10] Pietzka M A and Schuster J C 1996 *J. Am. Ceram. Soc.* **79** 2321
[11] Schuster J C, Nowotny H and Vaccaro C 1980 *J. Solid State Chem.* **32** 213
[12] Hug G, Jaouen M and Barsoum M W 2005 *Phys. Rev.* B **71** 024105
[13] Sun Z, Ahuja R and Schneider J M 2003 *Phys. Rev.* B **68** 224112
[14] Wang J Y and Zhou Y C 2004 *J. Phys.: Condens. Matter* **16** 2819
[15] Sun Z, Ahuja R, Li S and Schneider J M 2003 *Appl. Phys. Lett.* **83** 899
[16] Sun Z, Music D, Ahuja R, Li S and Schneider J M 2004 *Phys. Rev.* B **70** 092102
[17] Teter D M 1998 *MRS Bull.* **23** 22
[18] Salama I, El-Raghy T and Barsoum M W 2002 *J. Alloys Compounds* **347** 271
[19] Kresse G and Hafner J 1993 *Phys. Rev.* B **48** 13115
[20] Kresse G and Hafner J 1994 *Phys. Rev.* B **49** 14251
[21] Kresse G and Joubert D 1999 *Phys. Rev.* B **59** 1758
[22] Monkhorst H J and Pack J D 1976 *Phys. Rev.* B **13** 5188
[23] Blöchl P E 1994 *Phys. Rev.* B **50** 17953
[24] Birch F 1978 *J. Geophys. Res.* **83** 1257
[25] Ye J, Hanada T, Nakamura Y and Nittono O 2000 *Phys. Rev.* B **62** 16549
[26] Shibata T, Bunker B, Mitchell J F and Schiffer P 2002 *Phys. Rev. Lett.* **88** 207205
[27] Reed J and Ceder G 2002 *Electrochem. Solid-State Lett.* **5** A145
[28] Armstrong A R, Robertson A D, Gitzendanner R and Bruce P G 1999 *J. Solid State Chem.* **145** 549
[29] Villars P and Calvert L D 1985 *Pearson's Handbook of Crystallographic Data for Intermetallic Phases* vol 2 (Metals Park, OH: American Society for Metals) p 1559